



## Nano-ceramics $Ti_3SiC_2$ Max phase reinforced single walled carbon nanotubes by spark plasma sintering

Badis Bendjemil<sup>1,2</sup>, Jamal Bougdira<sup>5</sup>, Faming Zhang<sup>3,4</sup>, Eberhard Burkel<sup>3</sup>

<sup>1</sup>LASEA, Dept of Chemistry, University of Badji-Mokhtar, 23000 Annaba, Algeria

<sup>2</sup>University of 8 Mai 1945 Guelma, 24000 Guelma, Algeria

<sup>3</sup>Physics of New Materials, Institute of Physics, 18055 Rostock, Germany

<sup>4</sup>School of Materials Science and Engineering, Southeast University, 211189 Nanjing, China

<sup>5</sup>Institut Jean Lamour, UMR 7198 CNRS - Université de Lorraine Faculté des Sciences et Technologies – BP 70239 F-54506 Vandoeuvre les NANCY cedex

Received 27 May 2015; Revised 12 April 2016; Accepted 19 April 2016

### Abstract

Ceramics titanium silicon carbide  $Ti_3SiC_2$  Max phase was rapidly synthesised and simultaneously consolidated by spark plasma sintering at which the extensive volume expansion occurred as a function of the temperature from ball milled SiC/Ti/C powders with Ti/SiC ratio of 3:1:2. The XRD patterns results were confirmed by FESEM observations and the EDAX analyses. The  $3Ti+1.2SiC+0.8C$  nano-ceramics were processed from  $3Ti+1.2SiC+0.8C/SWCNTs$  powders using spark plasma sintering (SPS) at temperatures of 1100, 1200 and 1300 °C with diting of SWCNTs from 0.0 to 1.0 wt% SWCNTs/ $Ti_3SiC_2$  nanocomposite. The effects of SWCNTs addition on phases, microstructure and hardness of the nanocomposite were investigated. The best product contained 1.0 wt% CNTs/  $Ti_3SiC_2/TiC$  which was sintered at 1300 °C, 60 MPa for 10 min The phase composition of the product could be tailored by adjusting the process parameters. The anisotropic hardness was observed in respect to the textured product.

**Keywords:** MAX phase;  $Ti_3SiC_2$ ; SPS; Mechanical properties; Microstructure-final; SWCNTs/ $Ti_3SiC_2$  nanocomposite, Texture.

**PACS:** 73.30.+y, 73.40.Ns, 73.40.-c.

### 1. Introduction

The fabrication of the ternary  $Ti_3SiC_2$  compound was carried out in a single step by PAS (Plasma Activated Sintering) starting from Ti, Si and graphite powders in a 3:1:2 molar ratio [1]. The synthesis/densification process was conducted under vacuum and consisted of two stages. During the first one, an electric pulsed current (10% on) of 100 A was applied for 99 s under a pressure of 34.5 MPa, while in the second stage, the current (non pulsed) was increased up to 1800–3500 A with an holding time in the range of 0–2 h and applied pressure in the range of 34.4–68.8 MPa. The maximum temperature values achieved were ranged from

\*) For Correspondence, Tel: +213673213352,  
E-mail: Badis23@ymail.com

1525 to 2500 °C. The optimal condition to give a nearly dense product characterized by density values of 4.53- 0.02 g/cm<sup>3</sup> very close to the reported theoretical value of 4.531 g/cm<sup>3</sup>, and containing small amounts (2 mol%) of TiC as a second phase, was a temperature of 1525 °C maintained for 2 h as well as an applied pressure of 34.4 MPa. Dense samples synthesized in this study were examined by optical and electron microscopy. The maximum size in the elongated dimension of these grains is about 25 nm, which is smaller by a factor of four than the average grain size (100 nm) reported for samples produced by HIPing at 1600 °C for 4 h [1]. Numerous papers on the synthesis and characterization of  $\text{Ti}_3\text{SiC}_2$ -based materials by means of the PDS technique were published by a Japanese research group [2–11].

Specifically, this ternary compound was first synthesized by reacting a Ti, SiC, and TiC powder mixture in the 4:2:1 molar ratio [2]. PDS process was conducted under vacuum at the temperature range of 1250–1450 °C for 15–120 min with a heating rate of 50–60 °C/min and 50 MPa mechanical pressure. The purity and density of the obtained  $\text{Ti}_3\text{SiC}_2$  product were higher than 92 vol.% and 99%, respectively, when the sintering temperature was higher than 1350 °C. At this latter value, the TiC content was almost constant in the sintering time interval of 15–120 min.

Regarding samples microstructure, it was found to be of three types, that is, fine, coarse and duplex grains, depending on the sintering temperature and time. Besides the already investigated Ti/SiC/TiC reactants, another powdered mixture, that is, Ti/TiSi<sub>2</sub>/TiC with 1:1:4 or 1:1:3 molar ratio was tested to synthesize the  $\text{Ti}_3\text{SiC}_2$  compound by PDS [3].

The process was carried out in a temperature range of 1100–1325 °C for 0–60 min, 50–60 °C/min heating rate and 50 MPa pressure. It was found that the formation of  $\text{Ti}_3\text{SiC}_2$  phase commenced at temperatures above 1200 °C. The obtained products consisted of the desired compound along with TiC as a second phase. In particular, when the sintering was conducted at a temperature near 1300 °C for 15 min, the maximum product purity for the 1:1:3 and 1:1:4 systems were about 93 and 95 wt.%, respectively. A good densification was achieved by the PDS technique, being the relative density of 1:1:3 and 1:1:4 samples higher than 99 and 98%, respectively, at sintering temperatures above 1250 °C. Moreover, a solid–liquid reaction mechanism between Ti–Si liquid phase and TiC particles was proposed to interpret the rapid formation of  $\text{Ti}_3\text{SiC}_2$ .

To synthesize  $\text{Ti}_3\text{SiC}_2$  samples, three further mixtures, that is, Ti/Si/C, Ti/SiC/C, and Ti/Si/TiC, were also processed by PDS [5–7].

Powder mixtures of Ti/Si/C with stoichiometric (3:1:2) and off-stoichiometric (3:1.05:2, 3.1:1:2, 3:1.15:2, 5:2:3, and 3:1.5:2) ratios were pulse discharge sintered in vacuum in a temperature range of 1200–1500 °C for 15–60 min, 50–60 °C/min heating rate and 50 MPa pressure [7]. It was found that the fabrication of high purity products was possible only when starting from nonstoichiometric powders, being the best product obtained with stoichiometric powders characterized by a  $\text{Ti}_3\text{SiC}_2$  content of only 65.2 wt.%. Conversely, when 5Ti/2Si/3C powders were sintered at 1300 °C for 15 min, the TiC content was reduced to about 6.4 wt.% and the corresponding relative density was approximately 99% of the theoretical value. When the 3Ti/SiC/C powder mixture was examined, it was found that the sintered material is characterized by a secondary TiC phase whose content is higher than 50 wt.% [7].

Finally, two Ti/Si/TiC powder mixtures with 1:1:2 and 2:2:3 molar ratios were subjected to PDS under the following operating conditions, that is, sintering temperature in the range 1200–1400 °C, dwell time 8–240 min, pressure of 50MPa, heating rate 50–60 °C/min [6–9]. With the aim of minimizing the amount of TiC in final products, it was found that the optimum sintering temperature was in the range of 1250–1300 °C. Correspondingly, the highest  $\text{Ti}_3\text{SiC}_2$  content was about 96–97 wt.% and higher than 99 wt.% for the cases of the 1:1:2 and 2:2:3 mixtures, respectively. In addition, when the PDS process was performed at

sintering temperatures above 1275 °C, the relative density of the obtained 2:2:3 samples was higher than 99%. Moreover, it was also found that the excess of Si in Ti/Si/TiC samples did not play a specific role in improving the purity of Ti<sub>3</sub>SiC<sub>2</sub> [9]. The product consists of large plate-shaped grains and small equiaxed grains and no secondary phases were identified. Thus, by summarizing the results above, the PDS (Pulse Discharge Sintering) method seems to represent a powerful tool for the fabrication of Ti<sub>3</sub>SiC<sub>2</sub>-based materials. Moreover, among the five different mixtures investigated by PDS, that one corresponding to 2Ti/2Si/3TiC led to the best Ti<sub>3</sub>SiC<sub>2</sub> product under the optimal sintering conditions of 1300 °C/ 15 min/50 MPa. Adapted from Sun et al. [7].

Coarse Ti particles (0.15 mm) were also successfully used for the synthesis of dense Ti<sub>3</sub>SiC<sub>2</sub> by PDS when starting from 2Ti/2Si/3TiC powder mixtures [11]. In particular, a 99% dense product with 97.8 wt.% purity was synthesized at 1450 °C for 20 min under an applied pressure of 50 MPa. More recently, to investigate the effect of Al addition on the synthesis of dense Ti<sub>3</sub>SiC<sub>2</sub> by PDS, powder mixtures of 3Ti/SiC/C/xAl (x = 0–0.2) were processed by the same group [12]. It was observed that small amount of Al addition favored both synthesis and consolidation of Ti<sub>3</sub>SiC<sub>2</sub>. In fact, an almost single-phase product was obtained if x = 0.15 or 0.2, when the sintering temperature of 1200 °C was held for 15 min. The various Ti<sub>3</sub>SiC<sub>2</sub> products obtained via PDS by the Japanese research group as described above have also been extensively characterized from the mechanical point of view in terms of deformation, fracture and cyclic fatigue propagation behavior, and the obtained results were reported elsewhere [10,13–15].

The rapid synthesis and consolidation of Ti<sub>3</sub>SiC<sub>2</sub> were performed by SPS (Spark Plasma Sintering) from the starting powders of Ti/Si/TiC mixed in a stoichiometric ratio of 1:1:2 [16]. The investigation was carried out in vacuum on a SPS-1050 machine (12/2 on–off time ratio) in temperature range 1125–1400 °C, 100 °C/min heating rate, 20–60 MPa pressure and 0–10 min holding time. Evidence of the Ti<sub>3</sub>SiC<sub>2</sub> formation was observed at about 1200 °C, at several hundreds degrees lower than the temperature of conventional reactive hot pressing. The optimal result was obtained at 1250 °C 60 MPa/10 min and corresponded to an almost fully densified product consisting of Ti<sub>3</sub>SiC<sub>2</sub> with 2 wt.% TiC.

Another Japanese research group has investigated the synthesis/ densification of Ti<sub>3</sub>SiC<sub>2</sub> taking advantage of the SPS apparatus [17–19]. Reactant powders used were made of TiC, Ti, carbon black. The effect of the Al addition on the synthesis process was investigated by SPS experiments which were performed at 80 °C/min heating rate, 30 MPa pressure, sintering temperature in the range 600–1400 °C for 0–30 min holding time. It was found that the appropriate addition of Al accelerated the formation of Ti<sub>3</sub>SiC<sub>2</sub> and favored its grain growth. Specifically, a 97.8% dense and pure Ti<sub>3</sub>SiC<sub>2</sub> product was obtained when the 3Ti/1Si/2C/0.2Al powder mixture was processed by SPS at 1150–1250 °C/30 MPa/10 min.

Also, the SPS products displayed a Vickers hardness of 4 GPa (at 1 N and 30 s). For the sake of comparison, the same powders were processed by HP (High Pressure) and similar products in terms of density and purity were obtained when sintering at higher temperatures and longer processing times, that is, 1300–1400 °C/30 MPa/2 h. More recently, the influence of Al addition to 3Ti/Si/2C powders on the fabrication of dense Ti<sub>3</sub>SiC<sub>2</sub> by SPS was further examined [20]. A SPS-2040 model apparatus was used in vacuum under the condition of 50 MPa mechanical pressure, 100–200 °C/min heating rate, 1100–1350 °C temperature, and 2–36 min holding time. It was found that dense Ti<sub>3</sub>SiC<sub>2</sub> materials (>98%) with TiC content less than 2 wt.% could be obtained from 3Ti/Si/2C/0.2Al mixtures at 1280 °C when the holding time was higher than 6 min. Product purity was improved by increasing the holding time but it was accompanied by an increase in grain size.

Carbon nanotubes (CNTs) received a great deal of attention due to their superior mechanical and physical properties. In particular, multi-walled carbon nanotubes (MWCNTs)

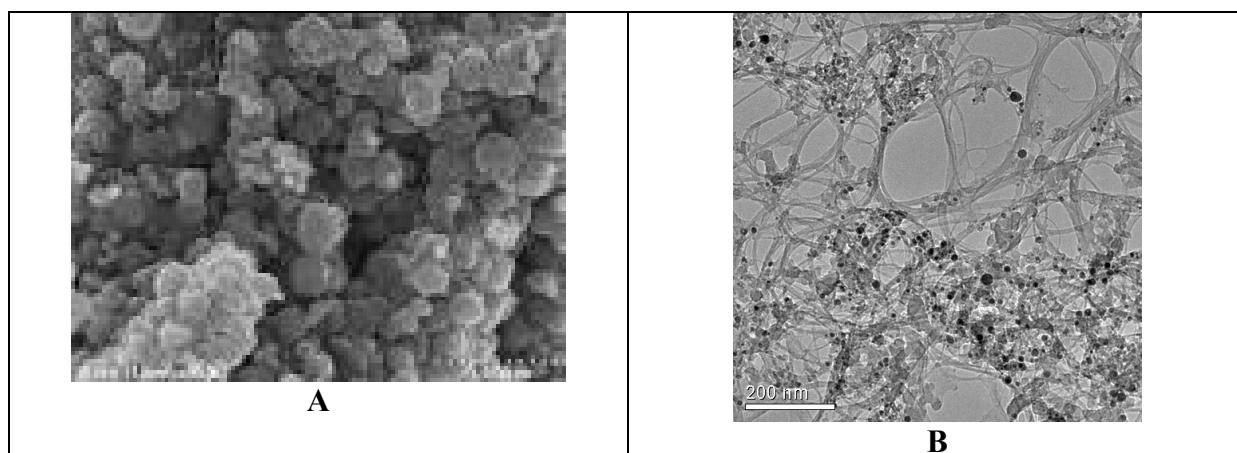
are expected to be used in industrial applications as their price has steadily decreased [22]. CNTs have been considered as useful and attractive additives to organic materials [23, 24], bulky metal [25], metallic coating [26], bulky ceramic [27] and ceramic coating [28] in order to improve the wear resistance and lower friction of mechanical components.

According to the theoretical consideration, a friction coefficient between the walls of MWCNTs should be extremely low. That is, MWCNTs have significant self lubricant property by nano-ball bearing effects [25]. It was reported [28] that the layered hexagonal MAX phases were thermodynamically stable nanolaminates displaying unusual and sometimes unique properties. Their layered nature suggested that they might have excellent promise as solid lubricant materials.

In our previous work, high-purity  $Ti_3SiC_2$  powders were synthesized successfully by SPS of Ti/SiC/C at temperatures as low as 1400 °C [5–7]. Dense polycrystalline  $Ti_3SiC_2$  of high purity was obtained by reactively hot isostatic pressing of Ti/SiC/C powders at 1300 °C, 60 MPa for 20 mn. Based on these results, in combination with the advantages of the SPS process, the purpose of this study is to obtain high-purity and dense  $Ti_3SiC_2$  with a fine-grained structure at lower temperatures in a short time. The synthesis and densification behavior of  $Ti_3SiC_2$  during the SPS were obtained. The reinforcement of  $Ti_3SiC_2$  matrix nano-ceramics with adding of 1.0 wt% SWCNTs process, as well as the microstructure development, were studied. Several mechanical properties were also measured.

## 2. Experimental Procedure

Commercially available powders of Ti (<45  $\mu$ m, 99.7 % purity, Sumitomo Sitix, Co. Ltd., Japan), SiC (<10  $\mu$ m, 99.9 % purity, High Purity Chemicals Co. Ltd., Japan), C graphite (1.7  $\mu$ m, 99.2 % purity, Nihon New Metals Co. Ltd., Japan) and SWCNTs with diameter of 1.2 nm were used as the raw materials (Fig. 1). The Ti, SiC, C and SWCNTs powders were mixed in a stoichiometric molar ratio of 1:1:2 in ethanol by SiC ball milling, and then dried in a vacuum. The mixtures were loosely compacted into a graphite die of 20 mm in diameter and sintered in the vacuum (1 Pa) at various temperatures (1100–1300 °C) using an SPS apparatus (Tycho SINTER, SPS-1050, Sumitomo Coal Mining Co. Ltd.,GERMANY) (Table 1, Fig.2). A constant heating rate of 100 °C/min was employed, while the applied pressure was 60 MPa. The on/off time ratio of the pulsed current was set to 12/2 in each run. The maximum current reached approximately 3000 A during sintering.



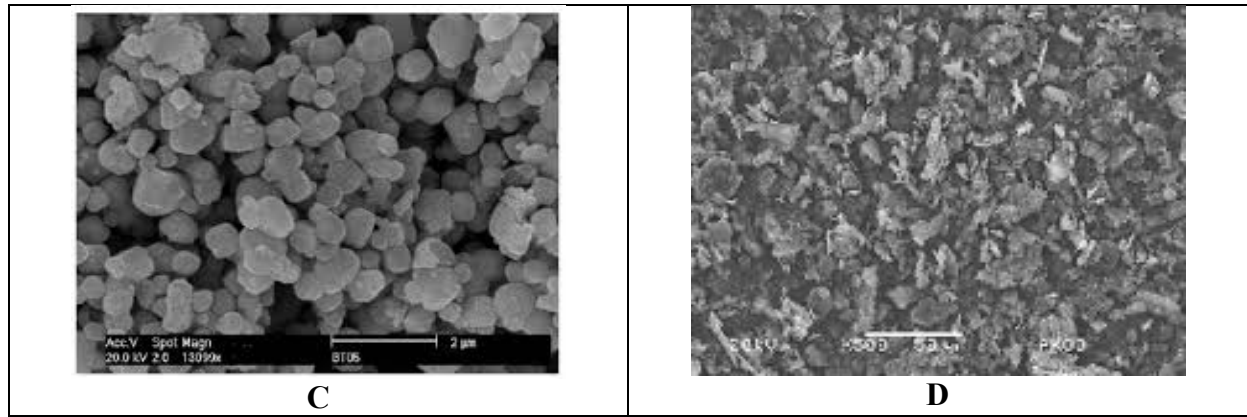


Fig. 1: Starting powders, **A.** SiC powder, **B.** Carbon nanotubes powder, **C.** Titanium powder **et D.** Carbon graphit powder

Table 1: Characteristics of the sintred samples

<b>Samples</b>	<b>T (C)</b>	<b>Time of the cycle (mn)</b>	<b>Heating rate (C/min)</b>	<b>P (MPa)</b>	<b>Ar (Sccm)</b>	<b>3Ti+1.2SiC+0.8C with wt% SWCNTs d=1.2 nm</b>	<b>Current (A)</b>
TSC	1300	20	100	60	200	00	3000
TSC <sub>1</sub>	1300	20	100	60	200	1.0	3000
TSC <sub>2</sub>	1200	20	100	60	200	1.0	3000
TSC <sub>3</sub>	1100	20	100	60	200	1.0	3000

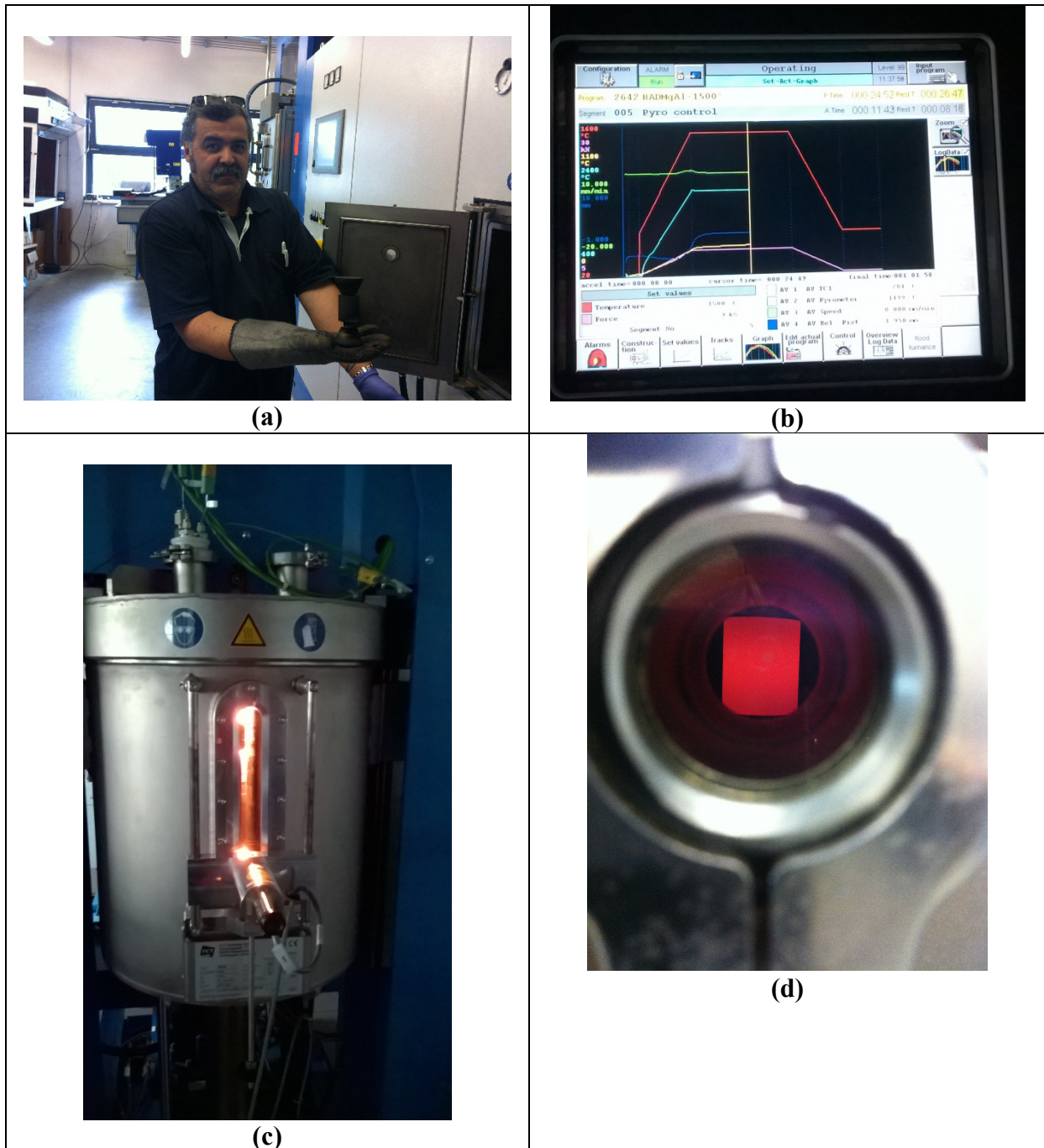


Fig. 2: Tycho SINTER, SPS-1050, Sumitomo Coal Mining Co. Ltd., **Rostock, Germany**,  
**a-** The researcher, **b-** Variation of the displacement, the displacement rate and the temperature in dependence of the heating time, **c- d-** The plasma produced by the current.

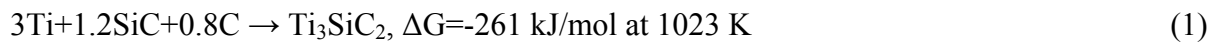
The soaking time at high temperatures was within 10 min. The upper ram of the SPS apparatus was fixed, while the displacement of the shifting lower press ram was recorded in order to analyze the synthesis and sintering behavior.

The sintered sample was polished and were evaluated by X-ray diffraction analysis using  $Cu K_{\alpha}$  radiation. The microstructure of the sample was observed by FESEM. The product was cut along the cylindrical axis into two pieces. The microhardness at the top surface and the lateral surface were measured by a diamond Vickers hardness tester. The indentation loads, ranging from 10 to 500 N, were applied for 15 s for each measurement.

### 3. Results and Discussion

#### 3.1. XRD analysis of powders and sintered Ti<sub>3</sub>SiC<sub>2</sub>/SWCNTs nanocomposites

Figure 2A, B, C and D show the XRD spectrum of the Ti<sub>3</sub>SiC<sub>2</sub>/TiC and the reinforced nanocomposite with 1.0 wt% SWCNTs at T= 1300, 1200 and 1100 °C, respectively. It can be seen that the main phase is the Ti<sub>3</sub>SiC<sub>2</sub> phase, and precipitated TiC coexist in the sintered samples. XRD patterns of the Ti<sub>3</sub>SiC<sub>2</sub>, and the nanocomposites are shown in Fig. 2A. The phases were formed during the sintering process in all of the samples because it is a thermodynamically favorable phase at the sintering temperature compared to Ti<sub>3</sub>SiC<sub>2</sub> phase [17]:



XRD spectrum of the nanocomposite, which indicates that the reaction between the Ti powders and SWCNTs did happen during the sintering process. This reaction has been previously observed [24], and it is considered that disordered carbons on wall defects and the open ends of the SWCNTs serve as carbon sources for interfacial reaction. The sintered samples consisted mainly of Ti<sub>3</sub>SiC<sub>2</sub> matrix, as major phases, and some secondary phases, such as TiC, appeared depending on the sintering temperature. X-ray diffraction patterns of sample (Ti<sub>3</sub>SiC<sub>2</sub>/TiC/1.0 wt% CNTs ceramic matrix nanocomposites sintered at 60 MPa pressure were enhanced because they are reinforced with the three phases, TiC and SWCNTs with higher intensity and is shown in Fig. 2B, C and D.

Fig. 2B shows the SWCNTs content at the sintering temperature of 1300 °C for 10 min at 60 MPa, which was reduced to 10 % when sintered at pressure because it reacted with Ti to produce Ti<sub>3</sub>SiC<sub>2</sub>, and TiC new reinforcement content was slightly increased.

Fig. 2A shows the XRD spectrum the top surface. The strongest diffraction peak changed from (104) plane on both surfaces to that of (008) plane on the pulverized sample. The peak intensity of (104) plane on the lateral surface is higher than that on the top surface.

The sample was cut along the cylindrical axis into two pieces. X-ray diffraction analyses on the top and lateral surfaces were carried out. The pulverized sample was also analyzed by X-ray diffraction. These results suggest that Ti<sub>3</sub>SiC<sub>2</sub> grains grew preferentially with the basal planes rotating towards the loading direction.

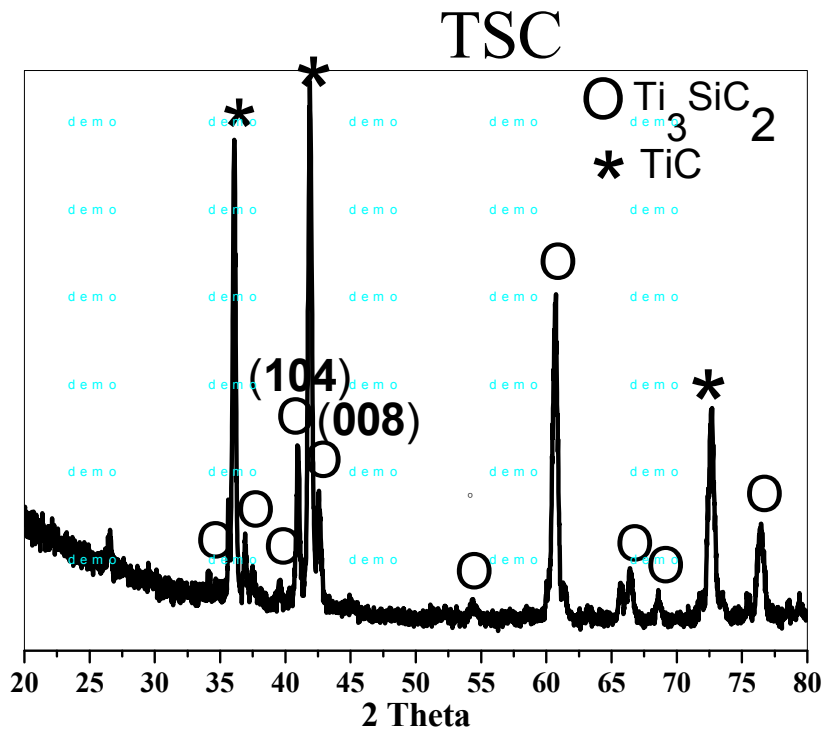


Fig. 3A

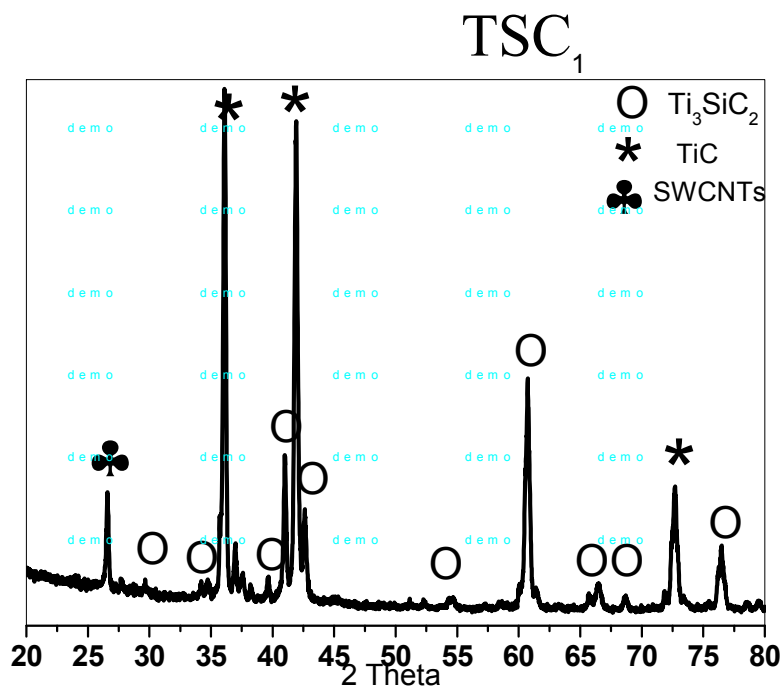


Fig. 3B



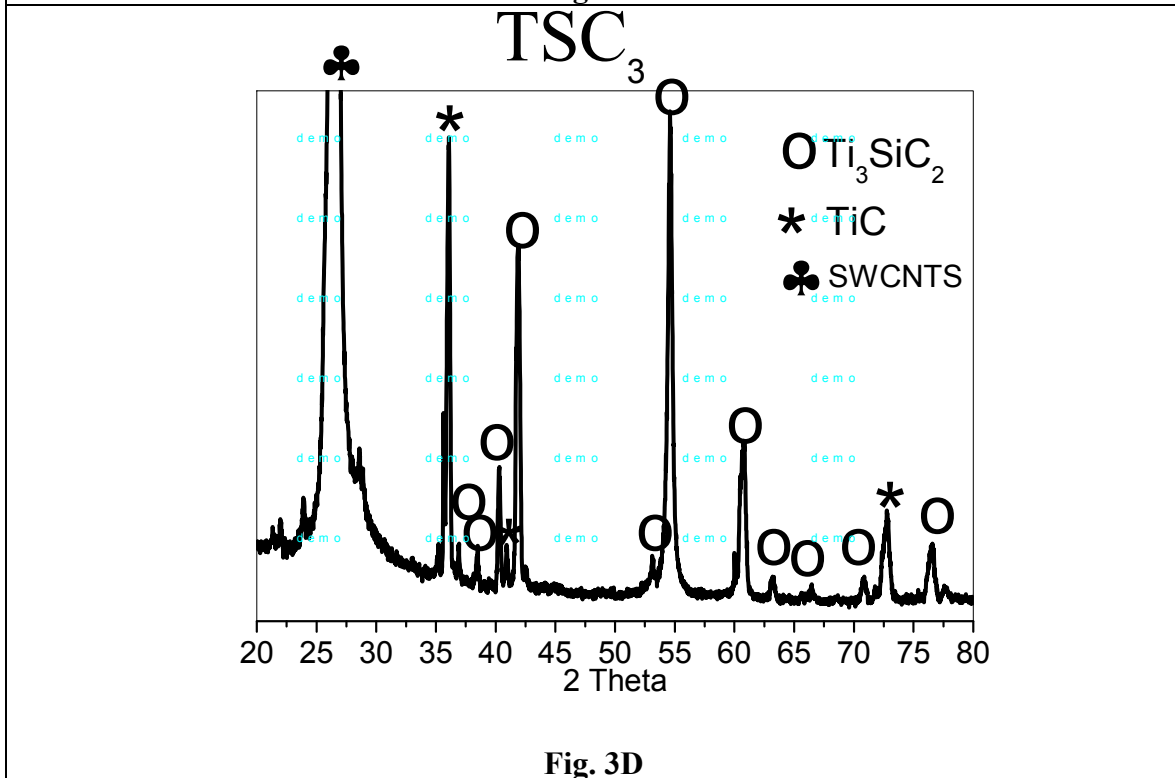
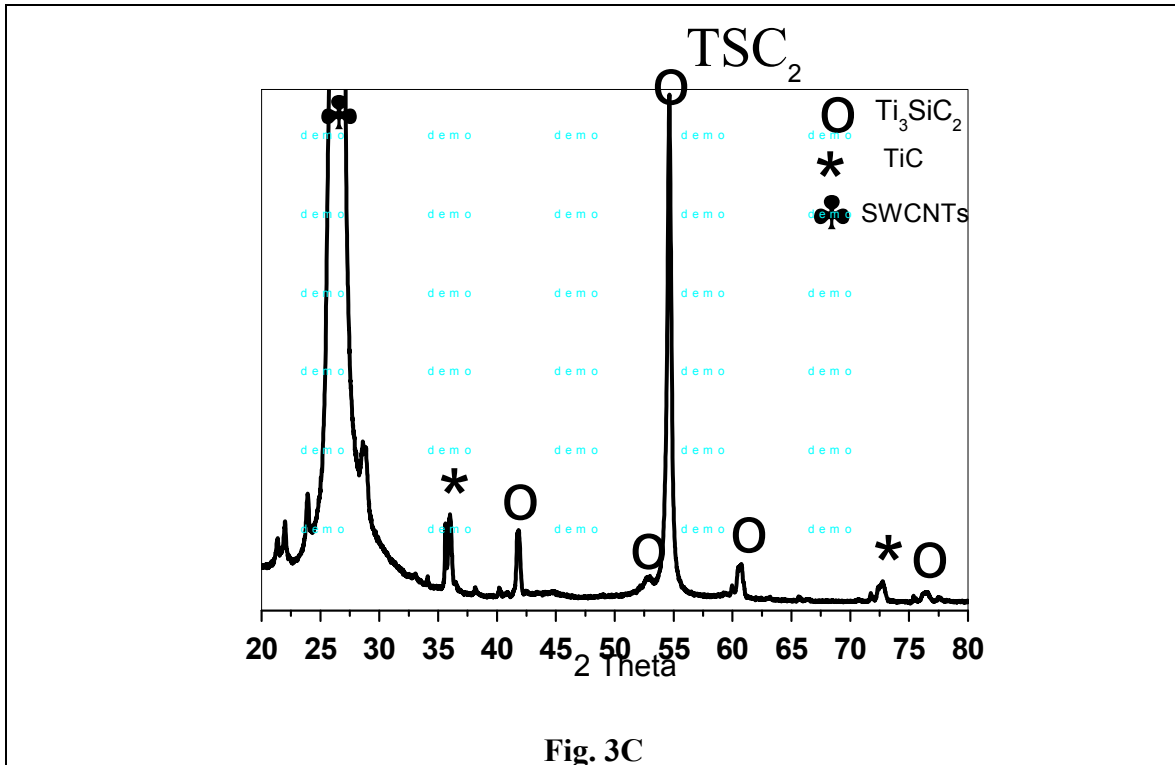


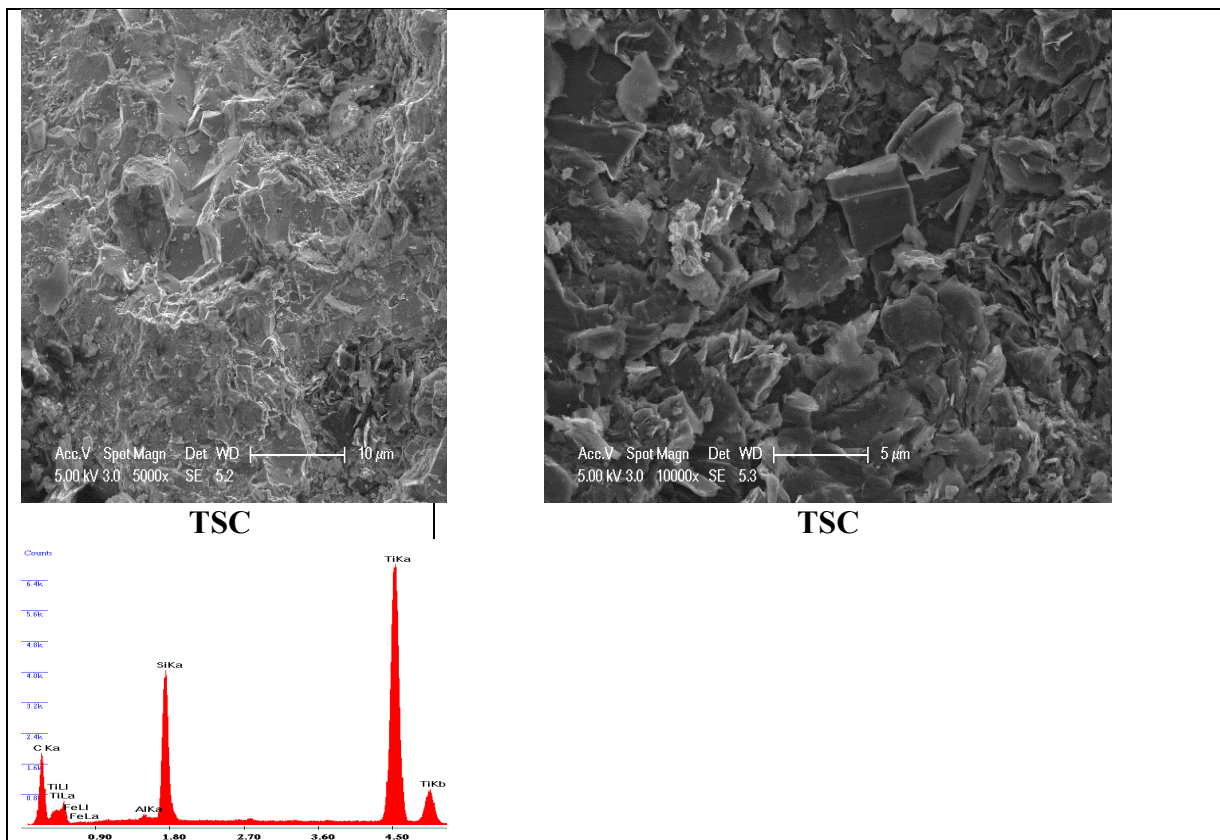
Fig. 3: X-ray diffraction spectrum on the top surface of the sintered samples using a 20-mm diameter die, **A.**TSC, **B.**TSC<sub>1</sub>, **C.**TSC<sub>2</sub>, **D.**TSC<sub>3</sub>.

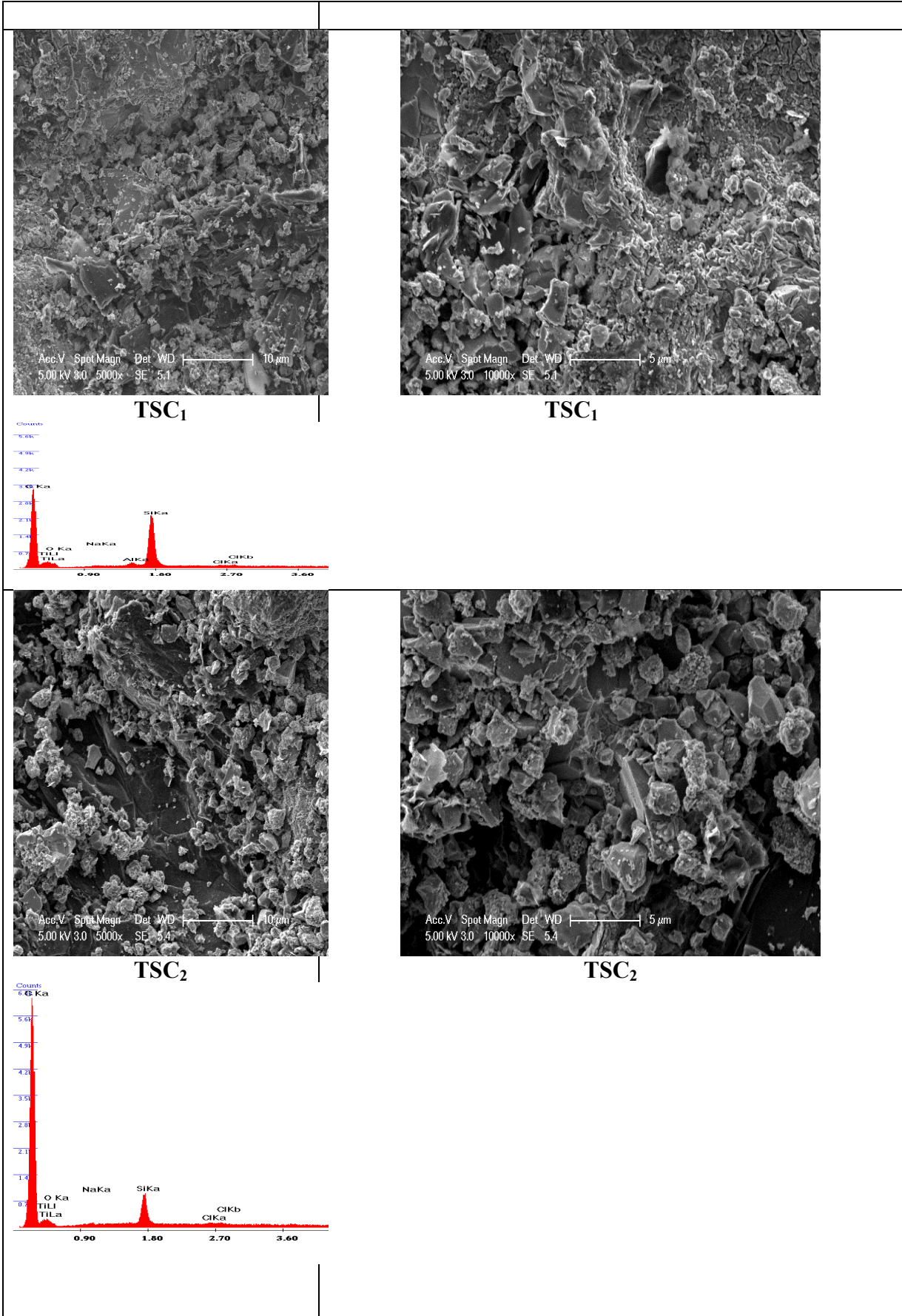
### 3.2. FESEM microstructural observation of sintered $\text{Ti}_3\text{SiC}_2/\text{TiC}/1.0$ wt% CNTs nanocomposites

The formation of  $\text{Ti}_3\text{SiC}_2$  seems to produce this volume expansion. Fig. 3 shows the fine grained structure of the top surface for the sample sintered at 1300, 1200 and 1100 °C, respectively at 60 MPa for 10 min after etching by an HF:HNO<sub>3</sub> aqueous solution. The average grain size of  $\text{Ti}_3\text{SiC}_2$  is below 10 μm. TiC (shown as a bright contrast is about 1–2 mm size, which is near the original TiC particle size in the as-received powders. Some closed pores inside the  $\text{Ti}_3\text{SiC}_2$  grains can also be seen, which would be attributed to the short sintering time. The  $\text{Ti}_3\text{SiC}_2$  typical grains have a thin plate-like form with a diameter of 10–30 mm and a thickness of 3–6 mm. These grain sizes are one order smaller than those of materials prepared by other methods.

FESEM analysis of the sintreed revealed the plate-like structure of the  $\text{Ti}_3\text{SiC}_2$  materials is shown in the Fig.3 and shown several orientation of the grain with the plate-like structure, and gray contrast granular areas in between the bulk grains. Fig.3 is a higher magnification view that shows the heavy nature of the plates formed probably due to the shock consolidation process.

The worn surfaces and wear debris are compared in Fig.4. The Microstructural and EDS analysis displays elemental analyses of the various regions of the sintered samples  $\text{Ti}_3\text{SiC}_2/\text{TiC}$ , and the  $\text{Ti}_3\text{SiC}_2/\text{TiC}/1.0$  wt% CNTs nanocomposites in chemical composition (at.%) (Fig. 3). EDS spectra was used to determine the elemental composition of the different regions in the sample and are presented by the red spectra. The FESEM micrographs in Fig. 3 shows a dark phase that corresponds to the  $\text{Ti}_3\text{SiC}_2$  matrix Max phase, and TiC is represented by the agglomerat in cubique polycrystal form in addition to unreacted SWCNTs, TiSi is not detected.





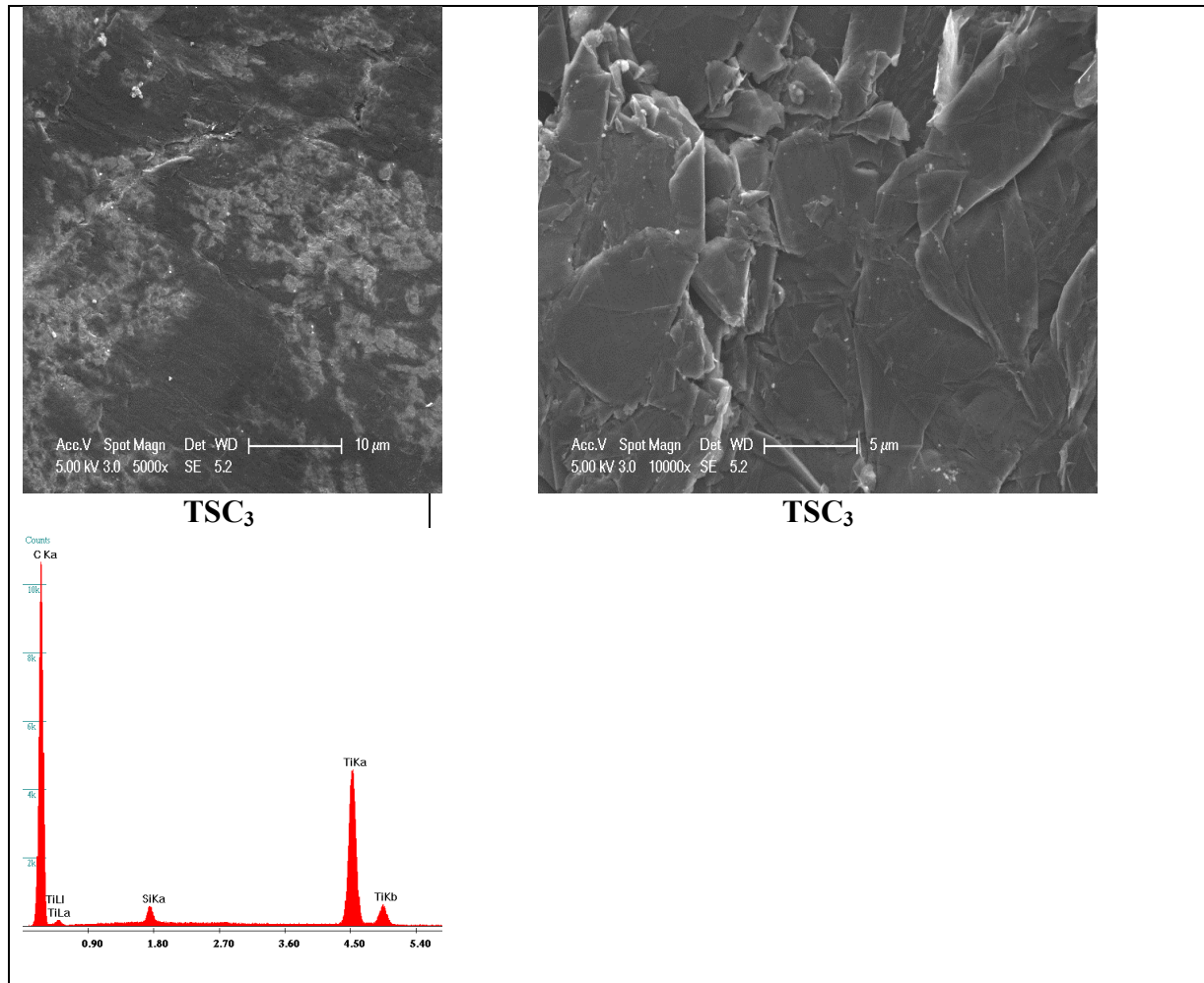


Fig. 4 : FESEM micrograph of the polished and etched surface for the sintered samples using a 20-mm diameter die.

### 3.3. Microhardness

According to the above results, it can be concluded that the wickers hardness has been improved by adding SWCNTs and enhanced at a high temperature. Fig. 4 shows the hardness as a function of the applied indentation load for the same sample. At higher loads, the microhardness reaches a constant value of 4.0 GPa for Max phase matrix or un-reinforced. The low hardness as indirect evidence of the purity of the as-synthesized  $\text{Ti}_3\text{SiC}_2$ . In the present study, the low hardness of the SPS synthesized sample containing 1.0 wt% SWCNTs at  $T=1100\text{ }^\circ\text{C}$  may be attributed to its low density (95% theoretical).

The hardness of the same sample exhibited an anisotropic behavior as shown in Fig. 4. On the top surface, the hardness, HV, decreased sharply at a load between 10 and 50 N and then decreased gradually at higher loads as already indicated in Fig. 4. On the lateral surface, the hardness, HV, showed less dependence on the indentation load and lower values than Hv at all load levels. Fig. 4 presents the variation of Vickers microhardness of  $\text{Ti}_3\text{SiC}_2/\text{TiC}/1.0$  wt% CNTs nanocomposites with CNTs reinforcement content and temperature. The microhardness of the composites increased almost linearly with increasing temperature at the SWCNTs reinforcement content. The hardness of SWCNTs (28–30 GPa) is nearly 7–8 times the previously reported values of hardness of  $\text{Ti}_3\text{SiC}_2$  (4 GPa). For the nearly single Max phase  $\text{Ti}_3\text{SiC}_2$  (SPS) sintered in this investigation, the microhardness was found to be 5.94

GPa (measured with indentation load of 10 N), which is higher than the previously reported hardness values for monolithic [22]. While the higher hardness of the  $\text{Ti}_3\text{SiC}_2$  sample could be due to a minor amount of SWCNTs phase in the  $\text{Ti}_3\text{SiC}_2$  sample, it could also be due to indentation size effects. It was reported that the hardness decreases with increasing load and asymptotically approaches a value of 2 GPa at higher loads. The microhardness in the range of about 2.5–3.5 GPa was found for lower loads (10 N). A slight increase in average hardness has been obtained from Max  $\text{Ti}_3\text{SiC}_2$  matrix nanocomposites prepared by sintering  $\text{Ti}_3\text{SiC}_2/\text{TiC}/1.0$  wt% CNTs nanocomposites reinforced with 1.0 wt% of SWCNTs with Ti and SiC elemental powders at  $T=1300$  °C exhibited highest hardness of about 6.5–8.5 GPa (Fig.4A). It is considered that in situ, TiC and the remaining SWCNTs act as reinforcements and play the major role in the improvement.

The best product contained  $\text{Ti}_3\text{SiC}_2/\text{TiC}/1.0$  wt% CNTs which was sintered at 1300 °C, 60 MPa for 10 min. The hardness of the product  $\text{Ti}_3\text{SiC}_2/\text{TiC}/1.0$  wt% CNTs decreases with decreasing temperature (Fig.4B), with this, the electrodischarge among powders may lead to self-heating and purification of the particle surface, resulting in activation of the formation for  $\text{Ti}_3\text{SiC}_2$ , the platelet grains are parallel to the (001) plane and perpendicular to the c-axis of the  $\text{Ti}_3\text{SiC}_2$  crystal structure. The platelet  $\text{Ti}_3\text{SiC}_2$  grains tended to be parallel to the pressing direction. The corresponding FESEM micrographs around the indentation marks at the top and lateral surfaces show the lateral cracks extension from the indentation mark on the top surface, but not in the case of the lateral surface. It is suggested that on the lateral surface, the indentation load may act as a force to delaminate the platelet  $\text{Ti}_3\text{SiC}_2$  in the weak Si bonding direction. Due to the energy dissipation in this process, a higher toughness and a lower hardness is exhibited on the lateral surface as a result of the anisotropy caused by the preferential grain growth.

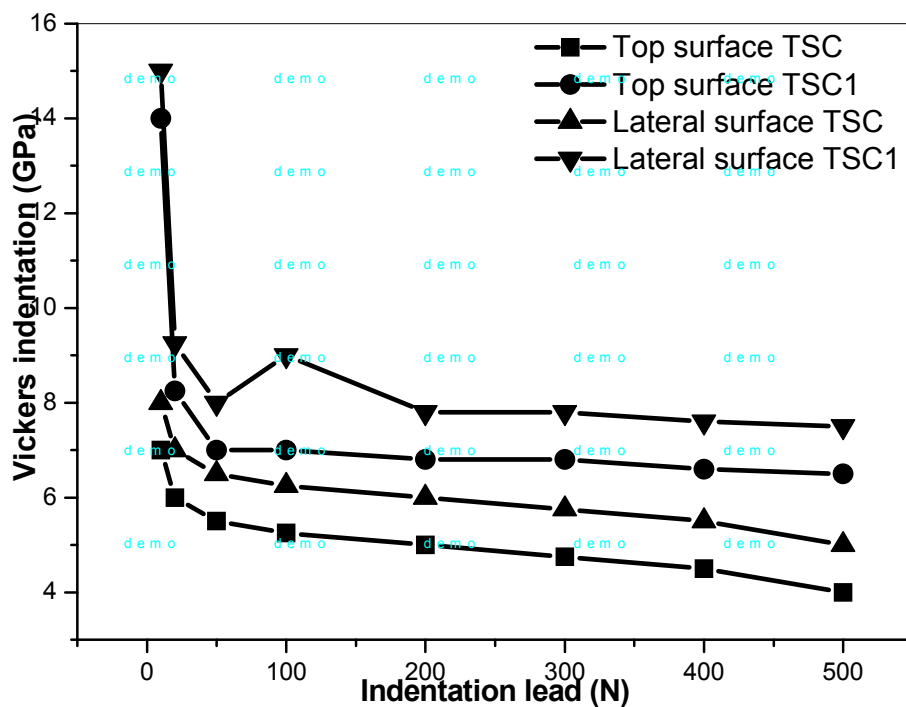


Fig. 5A

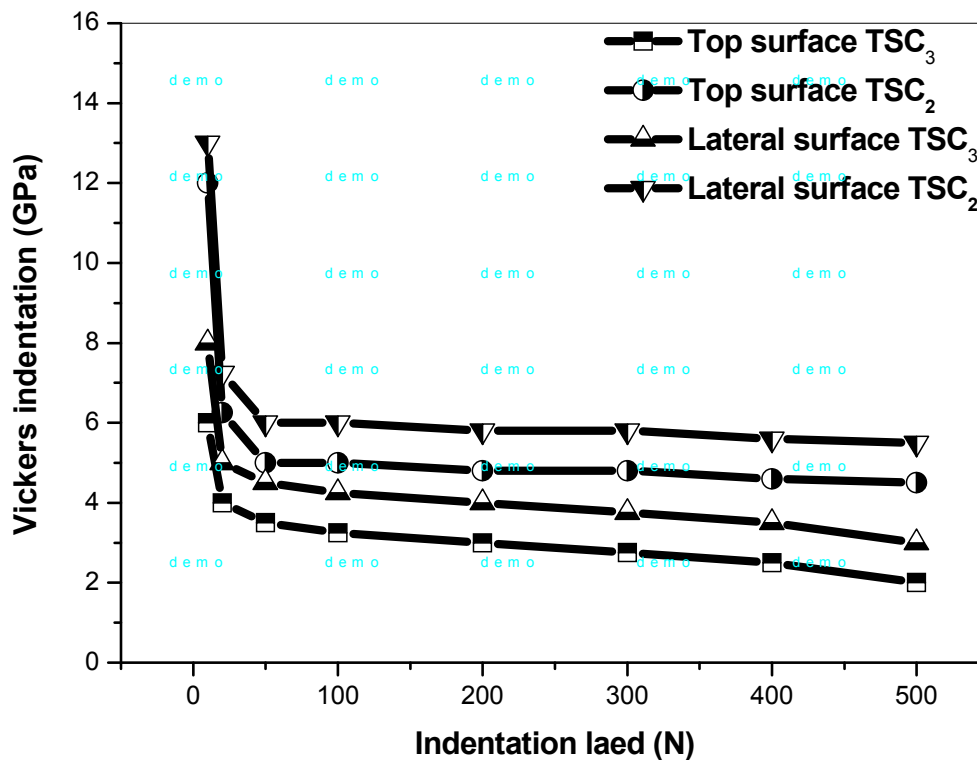


Fig. 5B

Fig. 5: Vickers hardness of as-synthesized samples using a 20-mm diameter die as function of indentation load, measured along two directions, **A.** TSC and TSC<sub>1</sub>, **B.** TSC<sub>2</sub> and TSC<sub>3</sub>

### 3.4. Relative density

The variation of the relative density of sintered  $\text{Ti}_3\text{SiC}_2/\text{TiC}$  and  $\text{Ti}_3\text{SiC}_2/\text{TiC}/1.0$  wt% CNTs nanocomposites with SWCNTs reinforcement is shown in Fig.5. The theoretical density of the composite used for obtaining relative density was calculated using a rule of mixture, using the densities of two constituent phase ( $\rho_{\text{Ti}_3\text{SiC}_2} = 4.53 \text{ g/cm}^3$ ,  $\rho_{\text{TiC}} = 4.50 \text{ g/cm}^3$ ,  $\rho_{\text{SWCNTs}} = 2.25 \text{ g/cm}^3$ ) with the given SPS processing parameters, the  $\text{Ti}_3\text{SiC}_2/\text{TiC}$  sample exhibited best densification with relative density greater than 99%, with the similar processing parameters and variation of temperature  $\text{Ti}_3\text{SiC}_2/\text{CNTs}$  nanocomposites. The relative density decreased with increasing temperature at the reinforcement of 1.0 wt% SWCNTs. The  $\text{Ti}_3\text{SiC}_2/\text{TiC}/1.0$  wt% CNTs nanocomposites at  $T=1300^\circ\text{C}$  exhibited relative density of about 98%. Clearly, the densification of the  $\text{Ti}_3\text{SiC}_2/\text{TiC}/1.0$  wt% CNTs decreases with decreasing temperature and reached the value of 96% at  $1200^\circ\text{C}$  and 94% at  $1100^\circ\text{C}$ . This seems to be the direct consequence of higher melting point of SWCNTs ( $T=3160^\circ\text{C}$ ) compared to that of  $\text{Ti}_3\text{SiC}_2$  ( $T=3000^\circ\text{C}$ ) and TiC ( $T=3000^\circ\text{C}$ ). XRD analysis indicated formation of new intermediate phase TiC from their action between Ti and C while the intensities of SWCNTs peaks remained unchanged. Depending on the final density to be achieved, the SPS operating condition were properly chosen, that is,  $750^\circ\text{C}$ , 5 Mpa for 5 min, to obtain a relative density of 75 %,  $800^\circ\text{C}$ , 25 Mpa for 5 min, for samples; 87 % dense, and  $850^\circ\text{C}$ , 50 Mpa for 5 min, for zero porosity compacts. The 13% porosity sample exhibited a round microstructure with high ductility, while the 25% porous product displayed much lower

stress flow as compared to that of the 13 % porosity [12]. Also, the easy sledding of their walls when attached by weak van der Waals force of coalesced MWCNTs can probably decrease the relative density. The density of the sintered samples was determined using the Archimedes water immersion method.



Fig.6: The measurement of the relative density

#### 4. Conclusion

Simultaneous synthesis and densification of Max  $Ti_3SiC_2$  was rapidly achieved by spark plasma sintering of Ti/SiC/C powder mixtures. Dense Max  $Ti_3SiC_2/TiC$  and Max  $Ti_3SiC_2/TiC/1.0$  wt% CNTs nanocomposites with varying temperature and 1.0 wt% SWCNTs weight fraction were fabricated by SPS at 1300, 1200 and 1100 °C under a pressure of 60 MPa for 10 min in pure Ar atmosphere protection. Max phase  $Ti_3SiC_2/TiC/1.0$  wt% CNTs at  $T=1300^\circ C$  had the highest Vicker's microhardness and relative density, which were HV 6.5 to 8.5 GPa and 98 %. Preferential grain growth of  $Ti_3SiC_2$  along the crystallographic basal plane was detected by XRD analysis. Because these platelet grains tended to align perpendicular to the loading surface, an anisotropic hardness was obtained. This increased with the addition of SWCNTs. Although TiC was formed by reaction of SWCNTs and Ti, unreacted SWCNTs could be found. Mechanical properties of  $Ti_3SiC_2/TiC$  were enhanced by unreacted SWCNTs at high temperature.

Further studies will be performed with variation of the graphite die diameter, to control the TiC content in the Max phase matrix. By spark plasma sintering, the extensive volume expansion as a function of the pressure will occur.

#### Acknowledgements

We are grateful to Prof. Jaafar Ghambaja, (Institut Jean Lamour, University of Henri Point Carré, Nancy, France) for his help in FESEM and XRD investigations.

## References

- [1] A. Feng, T. Orling, Z.A. Munir, *Mater. Res* **14** (1999) 925
- [2] Z.F. Zhang, Z.M. Sun, H. Hashimoto, T. Abe, *Scripta Mater* **5** (2001) 1461
- [3] Z.F. Zhang, Z.M. Sun, H. Hashimoto, *Adv. Eng. Mater* **4** (2002) 864
- [4] Z.F. Zhang, Z.M. Sun, H. Hashimoto, T. Abe, *Mater. Res. Innov* **5** (2002) 185
- [5] Z.F. Zhang, Z.M. Sun, H. Hashimoto, T. Abe, *J. Eur. Ceram. Soc* **22**( 2002) 2957
- [6] Z.F. Zhang, Z.M. Sun, H. Hashimoto, *Metall. Mater. Trans A***33** (2002) 3321
- [7] Z.M. Sun, Z.F. Zhang, H. Hashimoto, T. Abe,; *Mater. Trans* **43** (2002) 428
- [8] Z.F. Zhang, Z.M. Sun, H. Hashimoto, T. Abe,; *J. Am. Ceram. Soc* **86** (2003) 431
- [9] Z.F. Zhang, Z.M. Sun, H. Hashimoto, T. Abe; *J. Alloy Compd* **352** (2003) 283
- [10] Z.F. Zhang, Z.M. Sun, *Mater. Sci. Eng A* **408** (2005) 64
- [11] Y. Zou, Z.M. Sun, H. Hashimoto, S. Tada,; *Mater. Trans* **47** (2006) 1910.
- [12] Z.M. Sun, S. Yang, H. Hashimoto, *J. Alloy Compd* **439** (2007) 321
- [13] Z.M. Sun, Z.F. Zhang, H. Hashimoto, T. Abe, *Mater. Trans* **43** (2002) 432
- [14] ZF Zhang, ZM Sun, H Hashimoto, *Mater. Lett.* **57** (2003) 295.
- [15] H. Zhang, Z.G. Wang, Q.S. Zang, Z.F. Zhang, Z.M. Sun, *Scripta Mater* **49** (2003) 87
- [16] N.F. Gao, J.T. Li, D. Zhang, Y. Miyamoto, *J. Eur. Ceram. Soc* **22**. (2002) 2365
- [17] J. Zhu, B. Mei,; *J. Mater. Sci. Lett* **22** (2003) 889
- [18] J. Zhu, B. Mei, X. Xu, J. Liu, *Scripta Mater* **49**. (2003) 693
- [19] W. B. Zhou, B.C. Mei, J.Q. Zhu, *Mater. Lett* **59** (2005) 1547
- [20] J. Zhang, L. Wang, W. Jiang, L. Chen, *J. Alloy Compd* **437** (2007) 203
- [21] U. Anselmi-Tamburini, Y. Kodera, M. Gasch, C. Unuvar, Z.A. Munir, M. Ohyanagi, *Journal of Materials Science* **41** (2006) 3097
- [22] T. Kuzumaki, K. Miyazawa, H. Ichinose, K. Ito, *J. Mater. Res* **13** (1998) 2445
- [23] H. Kwon, M. Estili, K. Takagi, T. Miyazaki, A. Kawasaki, *Carbon* **47** (2009) 570
- [24] W.A. Curtin, B.W. Sheldon, *Today* **7** (2004) 44
- [25] G. Wei, Y. Jian, Q. Tai, Z. She-Ming, *Journal of Inorganic Materials* **25** (2010) 1081.
- [26] W.X. Chen, J.P. Tu, L.Y. Wang, H.Y. Gan, Z.D. Xu, X.B. Zhang, *Carbon* **41** (2003) 21527
- [27] S.I. Cha, K.T. Kim, S.N. Arshad, C.B. Mo, S.H. Hong, *Adv. Mater* . **17**(2005) 1377
- [28] D.H. Nam, S.I. Cha, B.K. Lim, H.M. Park, D.S. Han, S.H. Hong, *Carbon* **50**( 2012) 241